

**MAGNETOSTATIC EXTERIOR ELECTROMAGNETIC RESPONSE OF  
EMPTAC AIRCRAFT**

**Valdis V. Liepa**

**Radiation Laboratory  
Department of Electrical Engineering and Computer Science  
The University of Michigan  
Ann Arbor, Michigan 48109**

**prepared for  
Dikewood, Division of Kaman Science Corp.  
2800 28th Street  
Santa Monica, California 90405**

**February 1988**



## Abstract

Frequency domain magnetostatic surface current data are presented for the EMPTAC aircraft when excited in low frequency magnetic field. The data were measured on a 1:129.2 scale model of a Boeing 720B aircraft at the University of Michigan magnetostatic facility over 0.3 to 100.3 MHz range, corresponding to 2.3 to 776.3 KHz for full scale situation. Due to the self-resonance and presence of higher modes in the facility, we expect the data to be valid to about 400 KHz.

These data are provided to complement the previously measured EMPTAC response for plane wave incidence over 0.77 to 36.9 MHz.

## Contents

1. Introduction	3
2. Facility	4
3. Measurements and Data	7

## Preface

These are the first magnetostatic measurements made in the facility as a part of generating the exterior electromagnetic response data base of aircraft. It is our expectation that such measurements will be part of response measurements in future programs.

I wish to thank Dr. Dipak Sengupta and Mr. Joe Ferris who helped in initial design and construction of the facility. In this measurement program Mr. Martin Kuttner wrote the software and helped with the measurements and processing of the data. His assistance is appreciated.



## 1. Introduction

In addition to the regular scale model measurements that we perform in an anechoic chamber surface field measurement facility usually over 100 MHz to 4.7 GHz<sup>(1)</sup> and which provide full scale electromagnetic response data typically in 1 to 50 MHz range, the University of Michigan also has a Magnetostatic Facility<sup>(2)</sup> where scale model aircraft and other objects up to 2 feet in size can be measured for magnetic excitation from about 1 to 30 MHz. The exact frequency range still needs to be determined from the evaluation of the field mappings that were performed earlier<sup>(2)</sup> and the data measured on actual models such as presented here.

The results presented here complement the data that were measured on the EMPTAC scale model earlier by the University of Michigan<sup>(3)</sup>. In fact, the same scale model, 1:129.2 scale, was used and the measurement stations and excitations were selected from the previous matrix. For the magnetostatic measurements ten cases were selected which include:

- (a) 6 testpoints for H-perpendicular to fuselage (wing-to-wing)
- (b) 3 testpoints for H-parallel to fuselage
- (c) 1 testpoint H-vertical to fuselage

The ten data sets measured are also applicable to 15 other cases, making a total of 25 data sets into which these magnetostatic measurements can be incorporated.

---

<sup>1</sup>Lee, K.S.H. (ed.), "EMP Interaction: Principles, Techniques and Reference Data," AFWL-TR-80-402, pp. 267-276, December 1980.

<sup>2</sup>Liepa, V.V., D.L. Sengupta and T.B.A. Senior, "Magnetostatic Surface Field Measurement Facility," AFWL-TN-86-29, 1986.

<sup>3</sup>Liepa, V.V., and J-F Huang, "Exterior Response of EMPTAC Aircraft," AFWL Interaction Application Memo 43, 1987.

## 2. Facility

The magnetostatic facility that we have at the University of Michigan consists of four 4x8-foot 1/8-inch thick aluminum plates cut out in the center to provide spherical volume when butted together as shown in Figure 2.1. The spherical volume has a radius of 0.83 m (2.24 ft) and there are placed two (Helmholtz) coils made of 0.141 semi-rigid 50-ohm coax, each coil having four equally-spaced feed points. The working volume of the facility is about a 0.6 m (2 ft) diameter sphere within which the field is uniform to within  $\pm 5$  percent of the value at the center.

Whereas previously we had used a signal generator, power amplifier, pre-amplifier and a vector voltmeter to make these measurements, here we used a Hewlett-Packard 8753A network analyzer, plus a power amplifier and a pre-amplifier. Block diagram of the set-up is shown in Figure 2.2. The network analyzer which covers 0.3 MHz to 3 GHz range was operated 0.3 to 100.3 MHz. Signal from the analyzer was amplified and sent to the facility. There a small (3 mm diameter) current loop picks up a signal which is proportioned to the magnetic field and through a pre-amp sends it to the analyzer for amplitude/phase measurement.

The computer was used to control the analyzer and record, process, and plot the data.



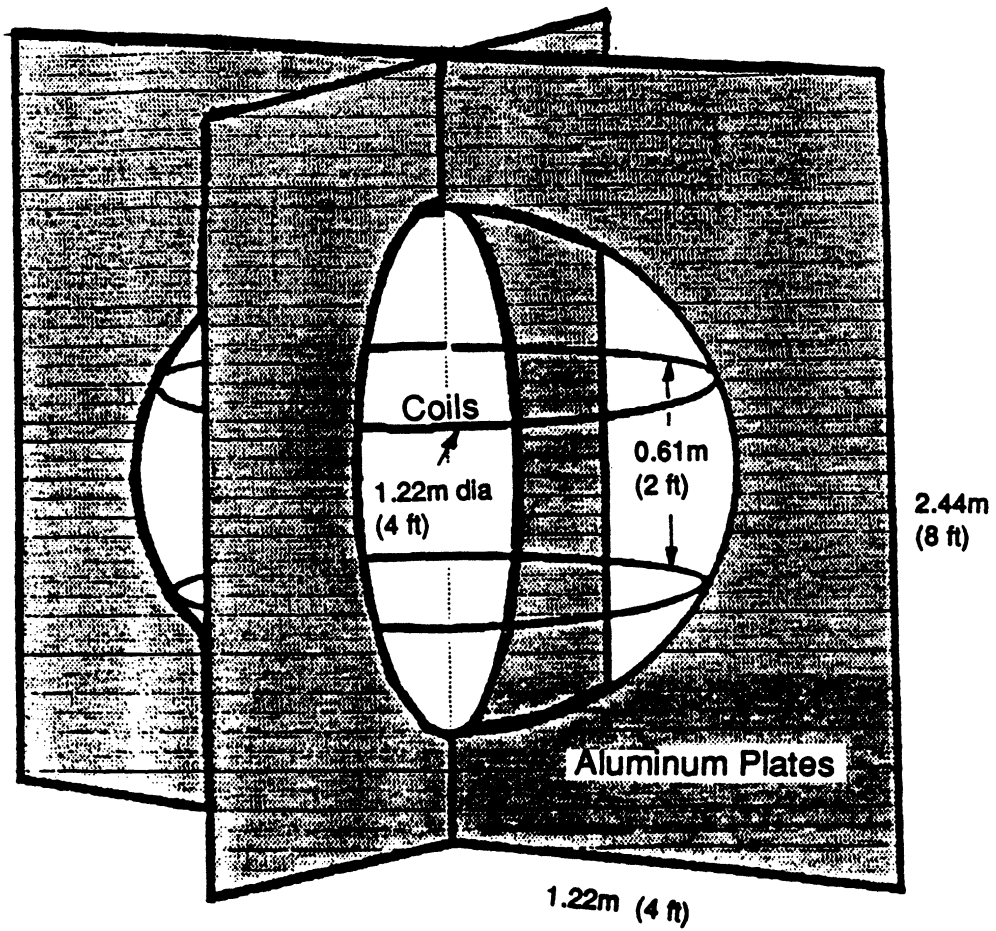


Fig. 2.1: Dimension of Magnetostatic Facility.  
The working area is about a 0.6 m (2 ft) sphere and magnetic field is vertical.

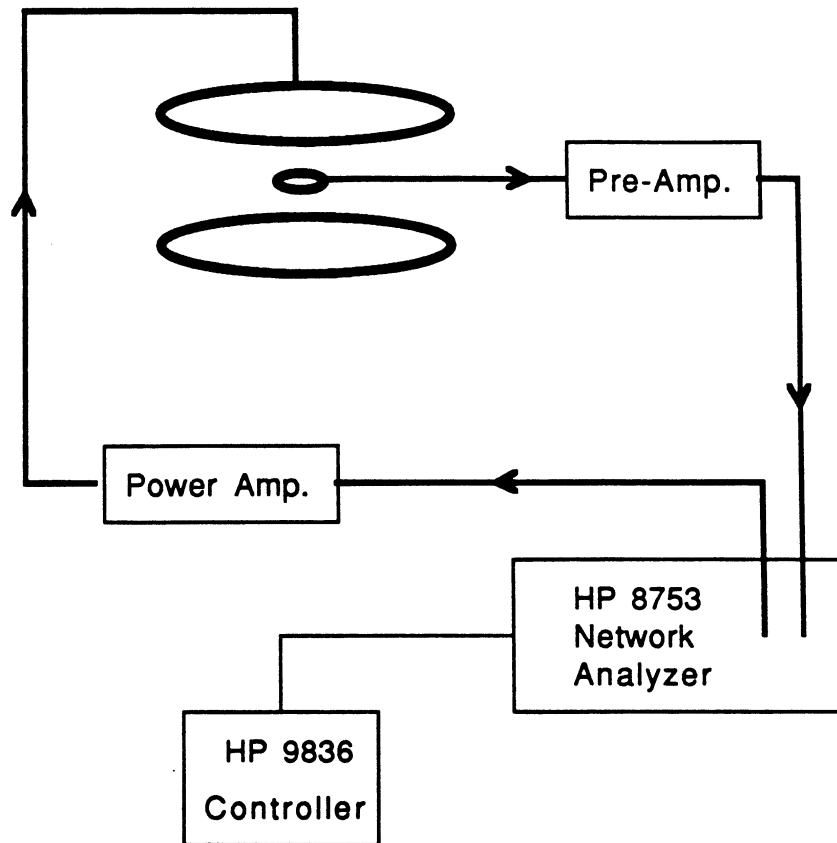


Fig. 2.2: Block diagram of equipment used.

### 3. Measurements and Data

In theory the measurements can be made by placing a model in the facility and measure voltage from the small loop probe that is positioned on the surface of the model. Then remove the model and measure the incident field with the same probe. The ratio of the two should then be the desired data. This works well on paper, but not in practice. In particular, there is over a 100 dB difference between the excitation signal and that coming from the small probe. Coupling through the cables, connectors and amplifiers can be appreciable and thus procedures needed to be worked out to remove undesirable signals either directly or when processing the data. Also, we have found that the measurement for the incident field with the probe on a sphere provides better calibration data than the direct measurement in free space.

To reduce the cross-talk signals all the cables were carefully made and routed as far apart as feasible to minimize coupling . In measurements the signal was measured twice: first with the loop oriented in normal direction and then with the loop rotated 180 degrees. The voltages induced in the loop by the magnetic field are then of opposite signs, but the voltage due to the coupling through the cables remain essentially the same (assuming nothing else is perturbed). This procedure was used on the model  $(V_{test}^+, V_{test}^-)$  and on the sphere  $(V_{cal}^+, V_{cal}^-)$ . Data were then processed using formula

$$J/H_o = \frac{V_{test}^+ - V_{test}^-}{V_{cal}^+ - V_{cal}^-} \cdot J_{sphere}$$

where  $J_{sphere}$  is current on the cal sphere computed from Mie series.

Figure 3.1 shows a photograph of current measurements on the model and the 7.958 cm (3.133 inch) diameter calibration sphere.

The magnetostatic measurements that were made are identified in Table 3.1 which also shows the measurements that were made over 100 to 4770 MHz (0.77 to 36.9 MHz full scale)<sup>(3)</sup>. The solid blocks indicate the cases for which the measurements were made and the dashed boxes indicate the cases for which these data also apply. We note that in the magnetostatic sense the direction of incidence is not applicable, only the direction of the exciting magnetic vector. Thus, the same data apply for the overhead incidence (H-parallel to the wings), the nose-on incidence (H-parallel to the wings), and the tail-on incidence, (H-parallel to the wings).

Figure 3.2 shows the excitation field and measured field components, and these are further described in Table 3.2. Measurement Stations are described in Table 3.3 and these are further described in reference (3).

The measured data that follows contain amplitude and phase normalized to the excitation field. Consider the data of Plot 1, FM5957. In Table 3.1 we see that the plot is for current  $J_A$ , STA:F520T, overhead incidence, excitation H-perpendicular to the fuselage (wing-to-wing). The top plot is magnitude and the lower is phase. The frequency axis is linear and the frequencies have been normalized appropriately for full scale aircraft. The amplitude is in dB, 2 dB/div; the reference is 0 dB and is identified by a tick mark along the left side of the plot. We see here the current amplitude is about 5.0 dB (1.78 linear) from 77 to 270 kHz and above 270 kHz (35 MHz measurement frequency) it starts to oscillate probably due to break-up of the excitation field in the facility. Below the 77 kHz (10 MHz) the amplitude appears to go to 0 dB

(1.0 linear); this is artifact of the finite thickness coating and is not representative of the real situation. This is consistent with the predictions for a coated model.<sup>(2)</sup> (Recall, the model is made of plastic, painted with silver paint, approximately 0.1 mm thick.) The corresponding phase is about 5 degrees over 77 to 270 kHz range and above 270 kHz (35 Mhz) breaks up, as did the amplitude.

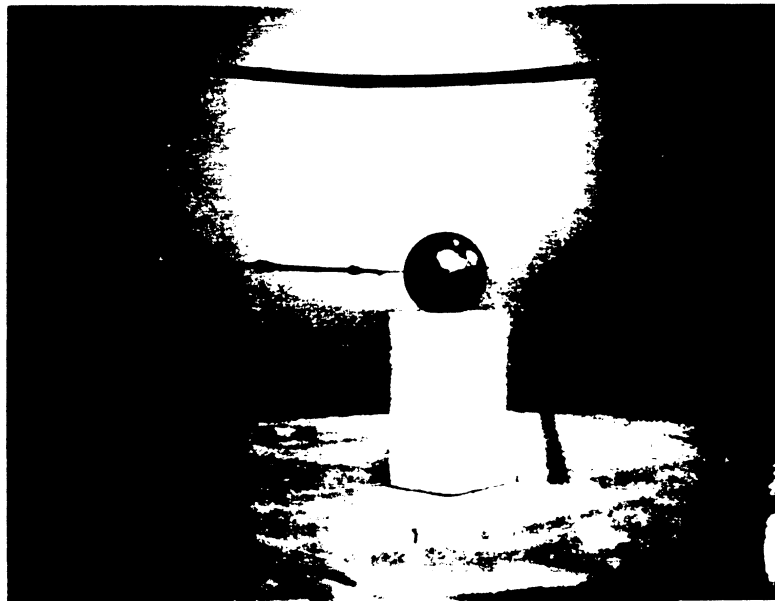
These data need careful scrutinizing before they are incorporated in the EMPTAC exterior response data base. The main questions that still need to be answered are:

- (a) up to what frequency are these data valid, and
- (b) what is the lower limit of the data

The first question (a) could be answered by mapping the fields of the facility at frequencies above those so far tested, that is, above 20 MHz. Making sample measurements in the facility on spheres and other known shapes and then carefully assessing the data is also suggested. The second question (b) can be answered by performing measurements on models with various coating thicknesses. A magnetic (nickel) coating such as used in EMI suppression may be an appropriate paint base material to consider for use in future measurements.



(a)



(b)

Fig. 3.1: Photograph of the model (a) and the 7.958 cm (3.133) inch cal sphere (b).

Table 3.1

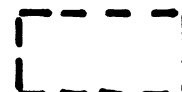
U of Mich 720B Measurements

Test Pt.	STA:	Overhead		Left Side-On		Nose-On	Tail-On
		$E_{  }, H_{\perp}$	$E_{\perp}, H_{  }$	$E_{  }, H_v$	$E_{\perp}, H_{  }$	$E_{vert}, H_{\perp}$	$E_{vert}, H_{\perp}$
1	F178	$Q$ FF6365		$Q$ FF6373		$Q$ FF6633	$Q$ FF6641
2	F520T	$J_A$ FF5957		$J_A$ FF6657		$J_A$ FF6073	$J_A$ FF6833
3	F520B	$J_A$ FF6009		$J_A$ FF6701		$J_A$ FF6125	$J_A$ FF6809
4	F800T	$J_A$ FF5965	$J_C$ FF6033	$J_A$ FF6665	$J_C$ FF6049	$J_A$ FF6201	$J_A$ FF6757
5	F800B	$J_A$ FF6017	$J_C$ FF6041	$J_A$ FF6709	$J_C$ FF6057	$J_A$ FF6233	$J_A$ FF6801
6	F1350T	$J_A$ FF5973		$J_A$ FF6673		$J_A$ FF6209	$J_A$ FF6765
7	F1350SR	$J_A$ FF6725 $Q$ FF6409		$J_A$ FF6273		$Q$ FF6425	$J_A$ FF6741
8	F1350B	$J_A$ FF6025		$J_A$ FF6717		$J_A$ FF6141	$J_A$ FF6773
9	V550L	$Q$ FF6473		$Q$ FF6501	$Q$ FF6533	$Q$ FF6525	
10	WL450T		$J_A$ FF6573		$J_A$ FF6557		
11	WL900T	$Q$ FF6309	$Q$ FF6601	$Q$ FF6317	$Q$ FF6433	$Q$ FF6449	$Q$ FF6609

measured case



applicable case



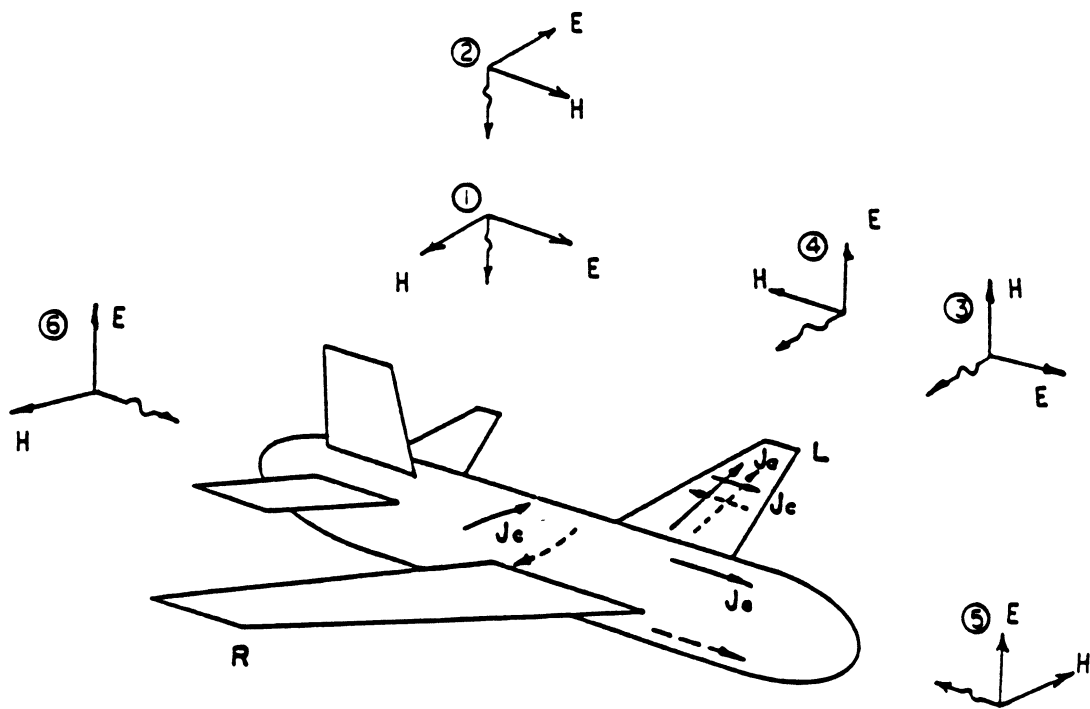


Fig 3.2: Excitation field and current directions measured on the model.  
The measured normal electric field is always outward.



**Table 3.2**

**EMPTAC Excitation Descriptions**

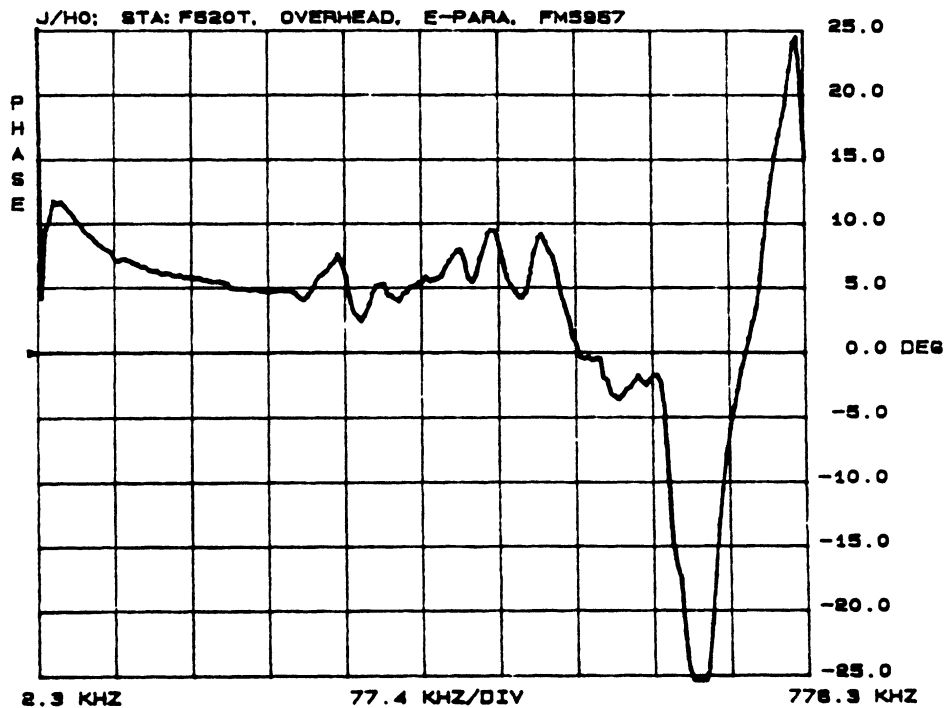
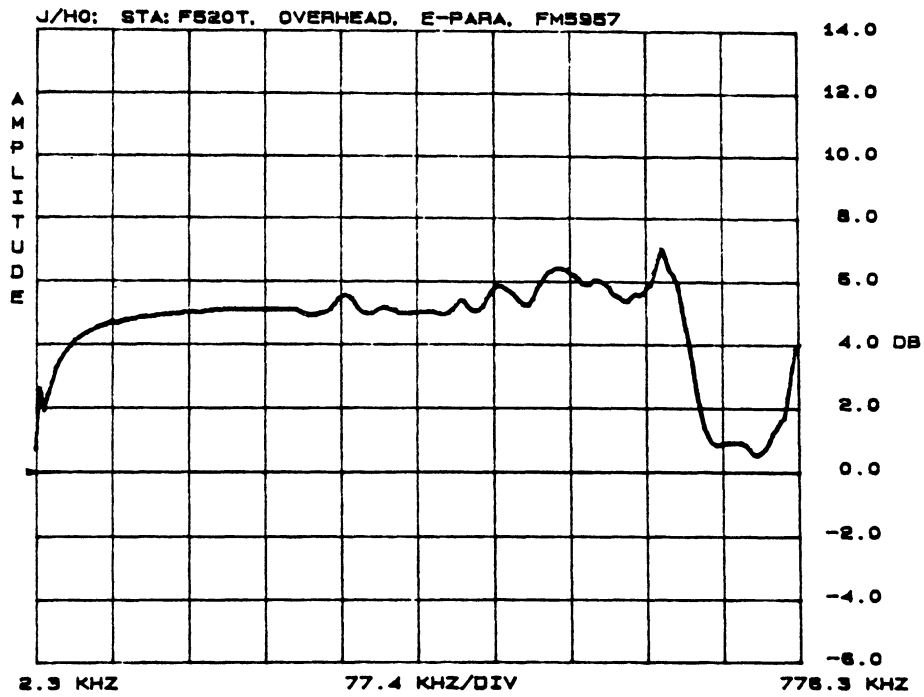
No.	Description
1	Top incidence, E parallel to fuselage; E direction from tail to nose
2	Top incidence, E perpendicular to fuselage; E direction from right to left wing
3	Left-side incidence, E parallel to fuselage
4	Left-side incidence, E vertical
5	Nose-on incidence, E vertical
6	Tail-on incidence, E vertical

See also Fig 3.2

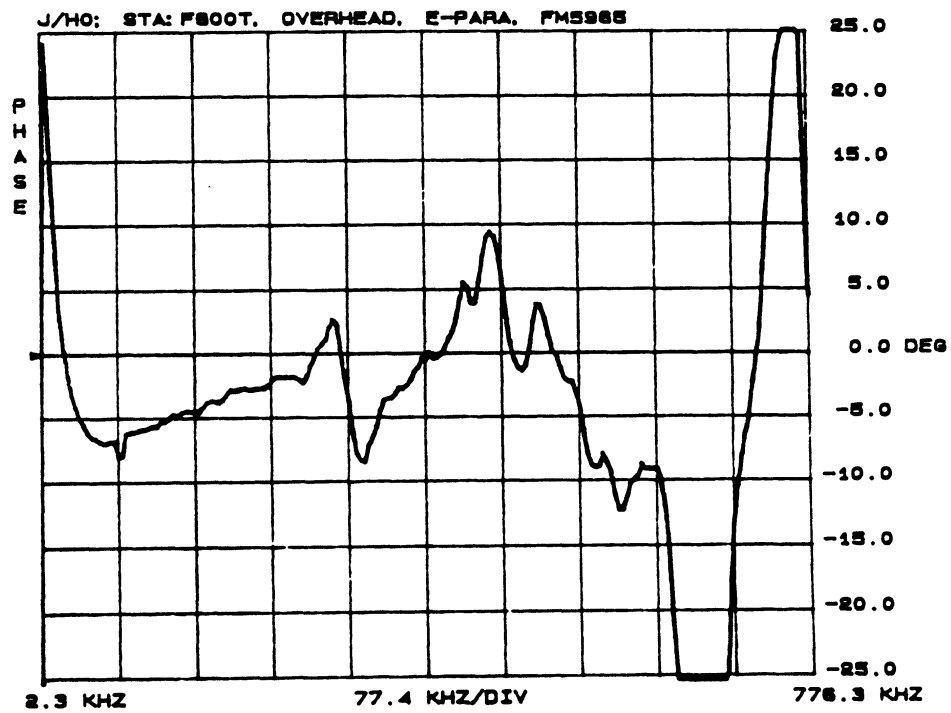
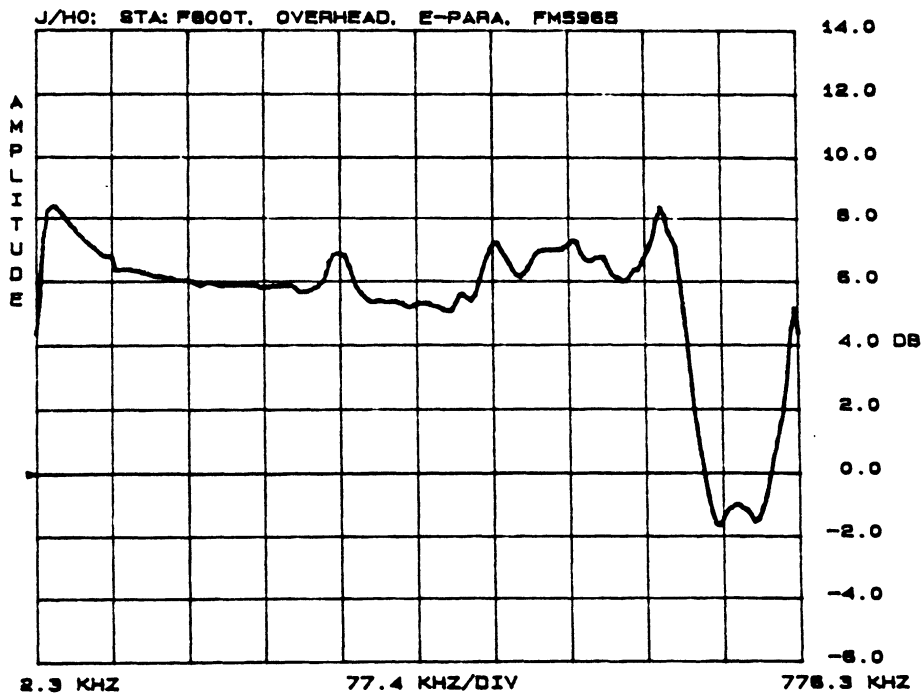
Table 3.3

EMPTAC Model Measurement Stations

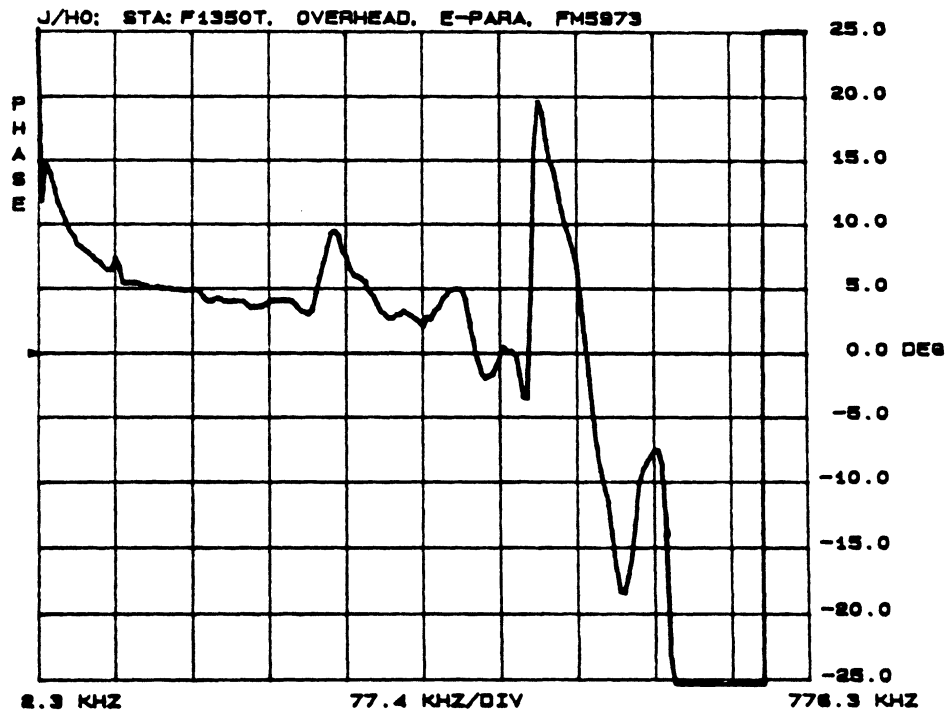
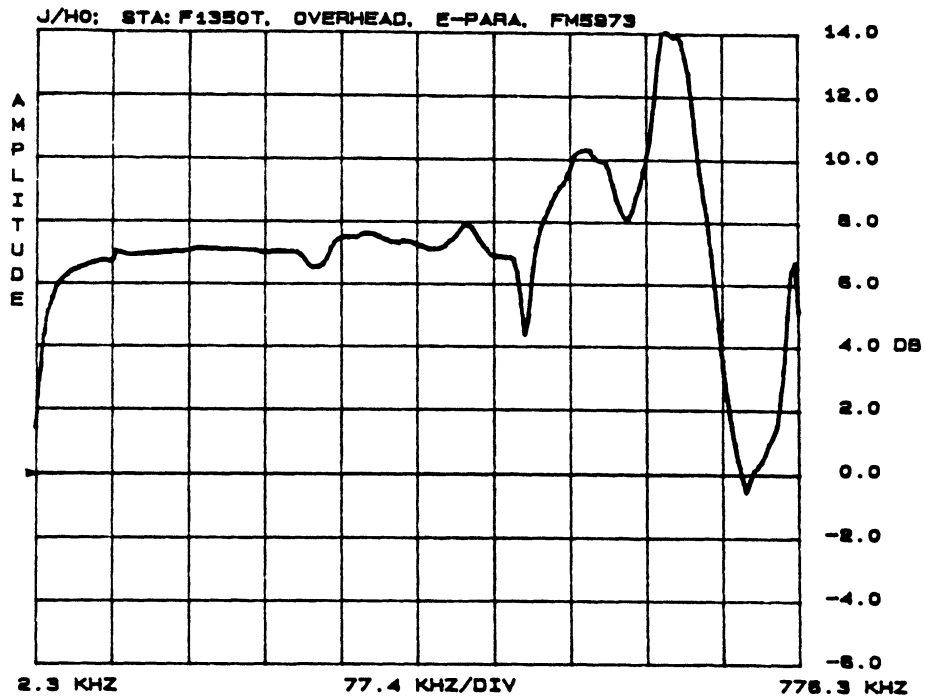
Test Pt.	Sta. No.	Location	Significance
1	F178	Fwd Bulkhead	Nose Cplg, Cockpit; Q
2	F520T	Fwd Fus, Top	Cockpit; J
3	F520B	Fwd Fus, Bottom	Nose Landing Gear; J
4	F800T	Wing-Fus Junc	Wing Root, Main Fus Cplg; J
5	F800B	Wing-Fus Junc	Landing Gear, Wing Root;J
6	F1350T	AFT Fus, Top	Main Fus Cplg; J
7	F1350SR	AFT Fus, Rt Side	Main Fus Cplg, Windows, Doors; J, Q
8	F1350B	AFT Fus, Bottom	Main Fus Cplg, Cargo Doors; J
9	V550L*	Vert Stab, Left	Empennage Coupling, Q
10	WL450T	Left Mid Wing, Top	Wing Coupling, J
11	WL900T	Left Wing Tip, Top	Wing Tip Coupling, Q



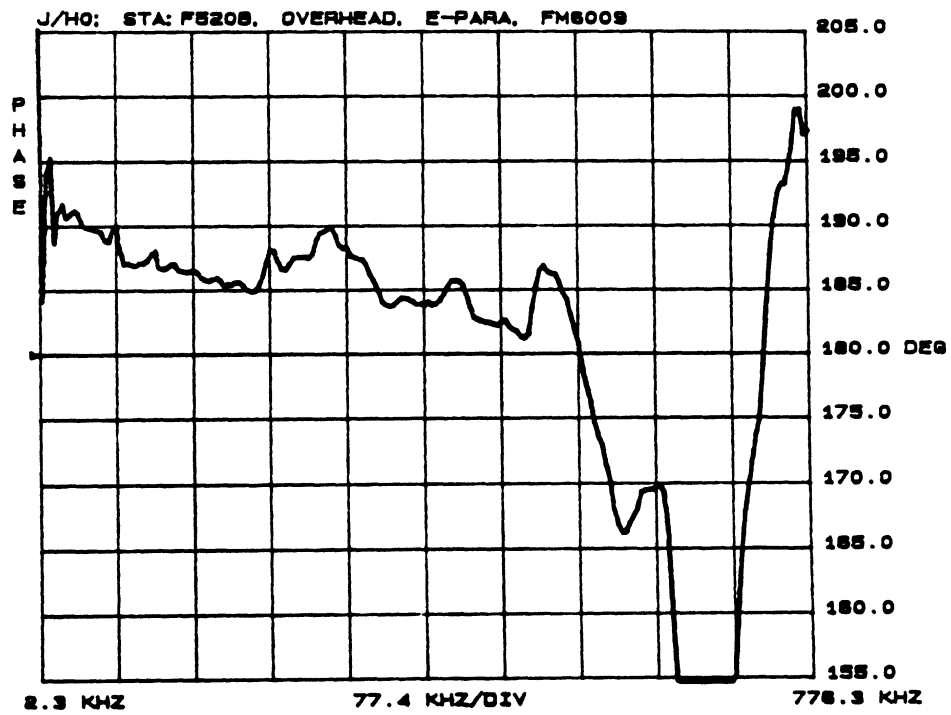
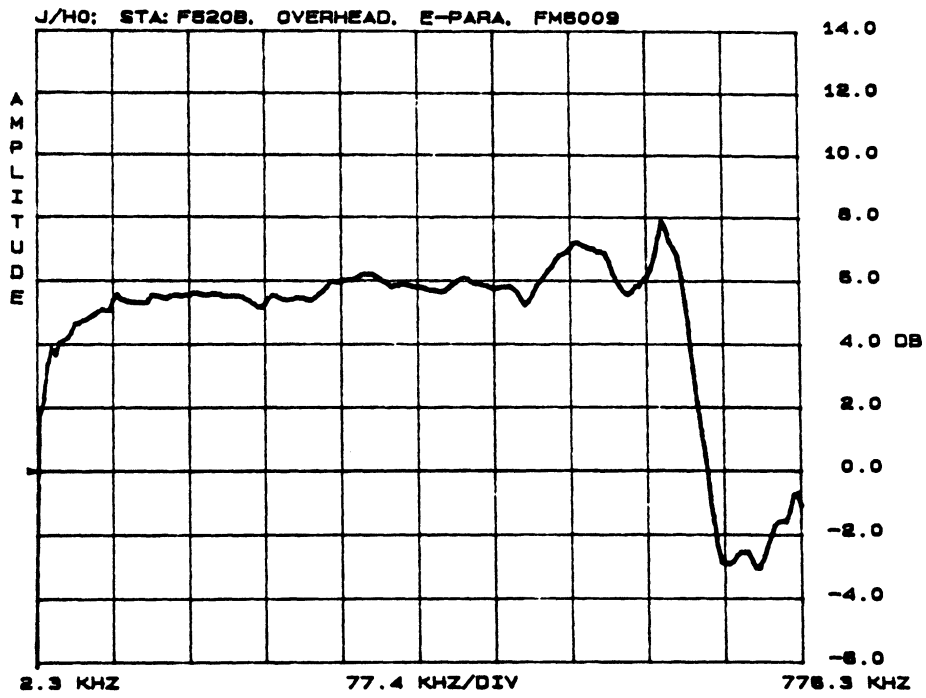
Plot 1. Current amplitude and phase at sta:F520T, overhead incidence, E-parallel to fuselage; FM5957.



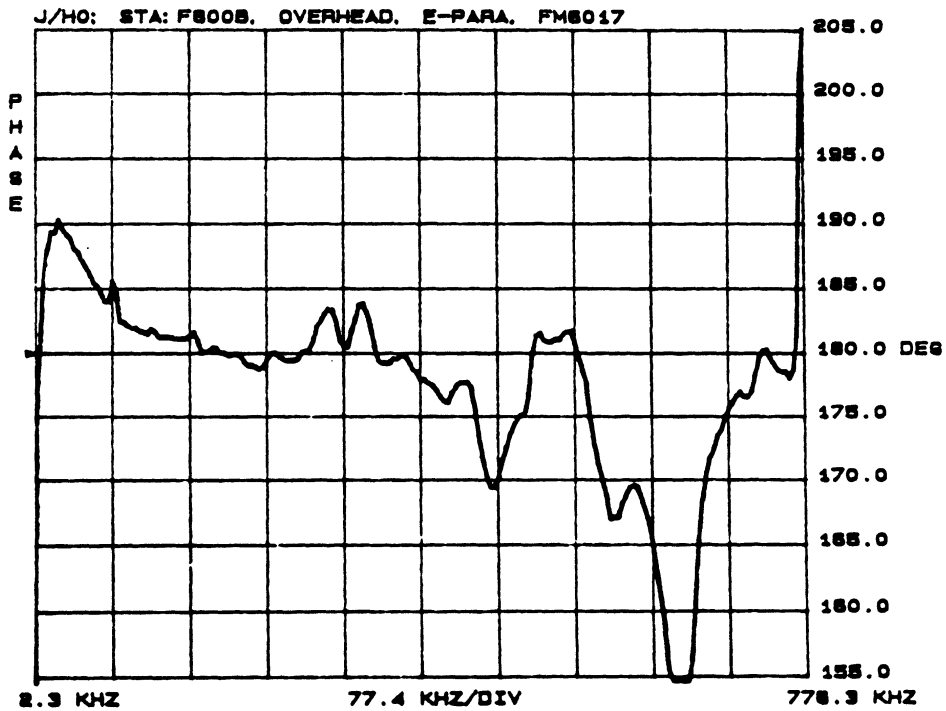
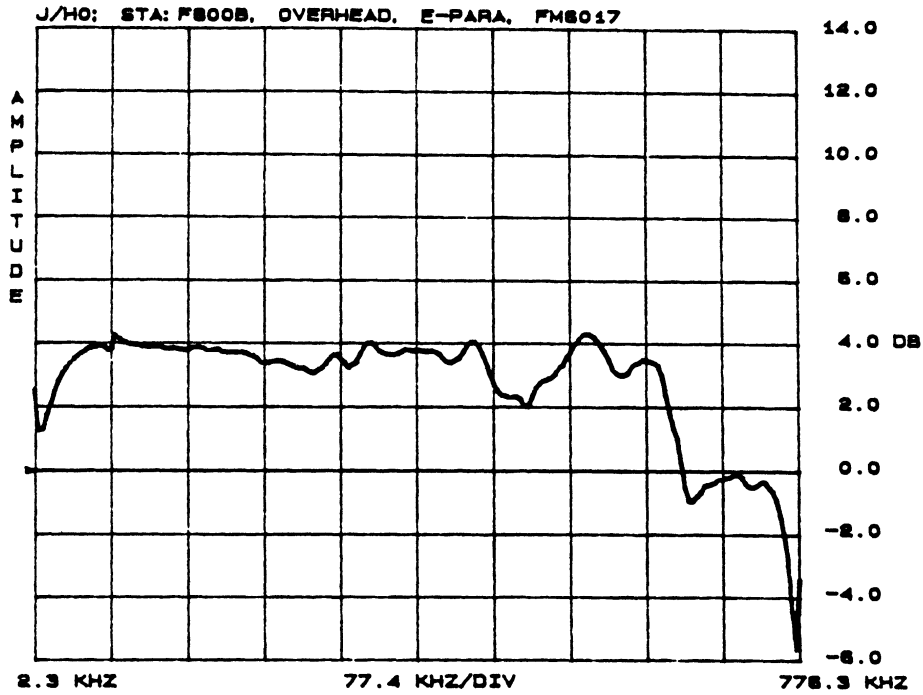
Plot 2. Current amplitude and phase at sta:F800T, overhead incidence, E-parallel to fuselage; FM5965.



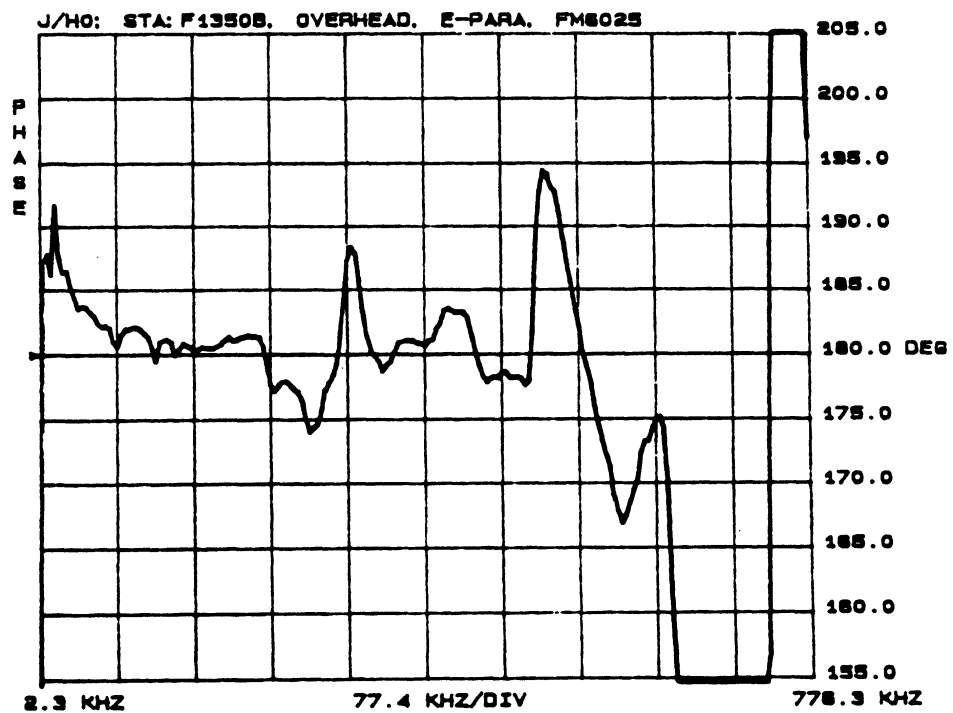
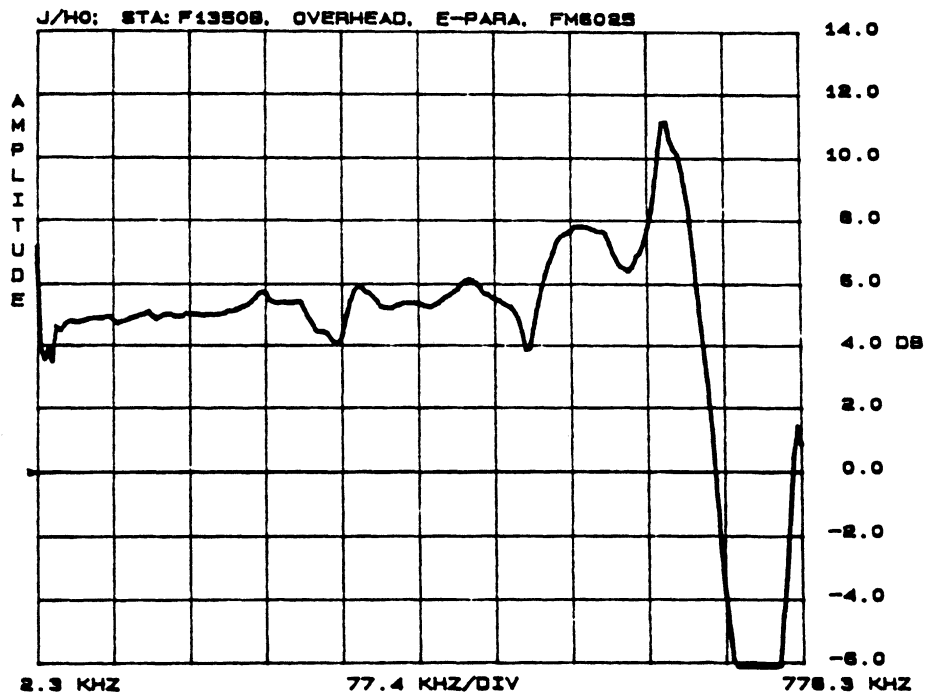
Plot 3. Current amplitude and phase at sta:1350T, overhead incidence, E-parallel to fuselage; FM5973.



Plot 4. Current amplitude and phase at sta: F520B, overhead incidence, E-parallel to fuselage; FM6009.

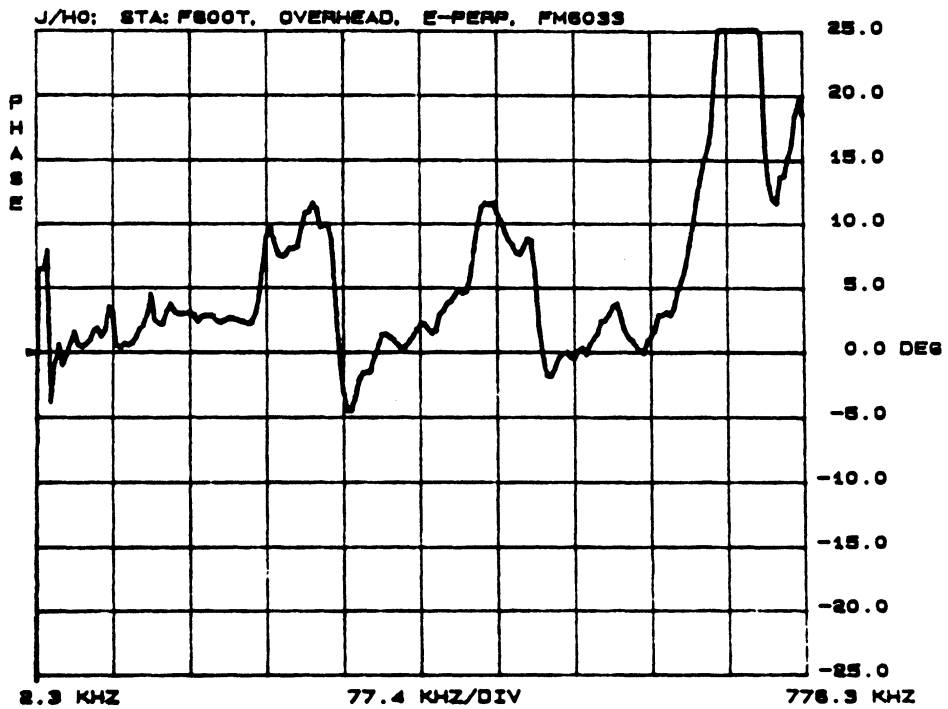
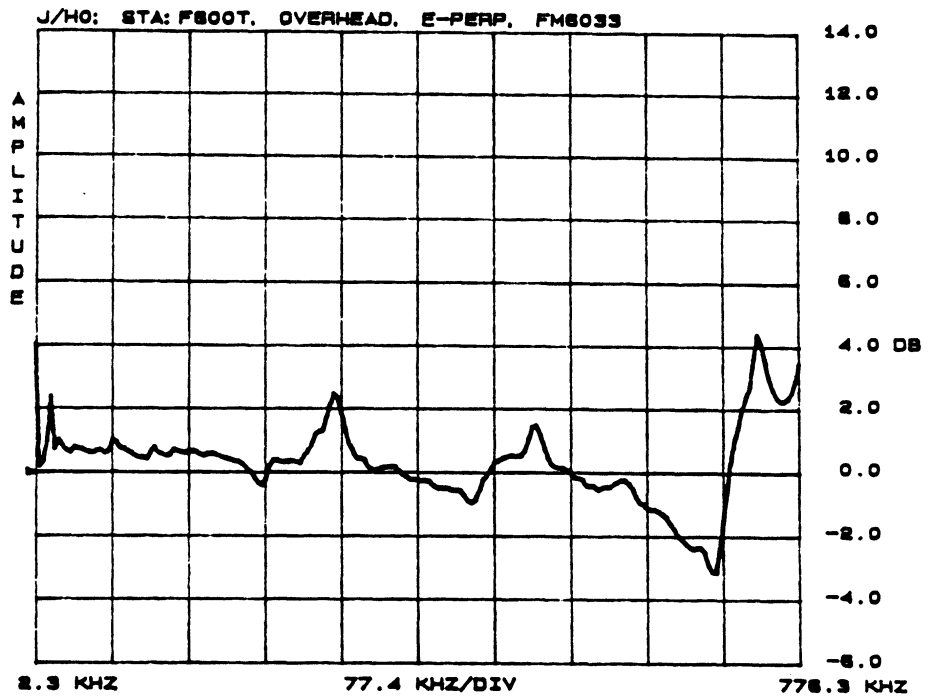


Plot 5. Current amplitude and phase at sta:F800B, overhead incidence, E-parallel to fuselage; FM6017.

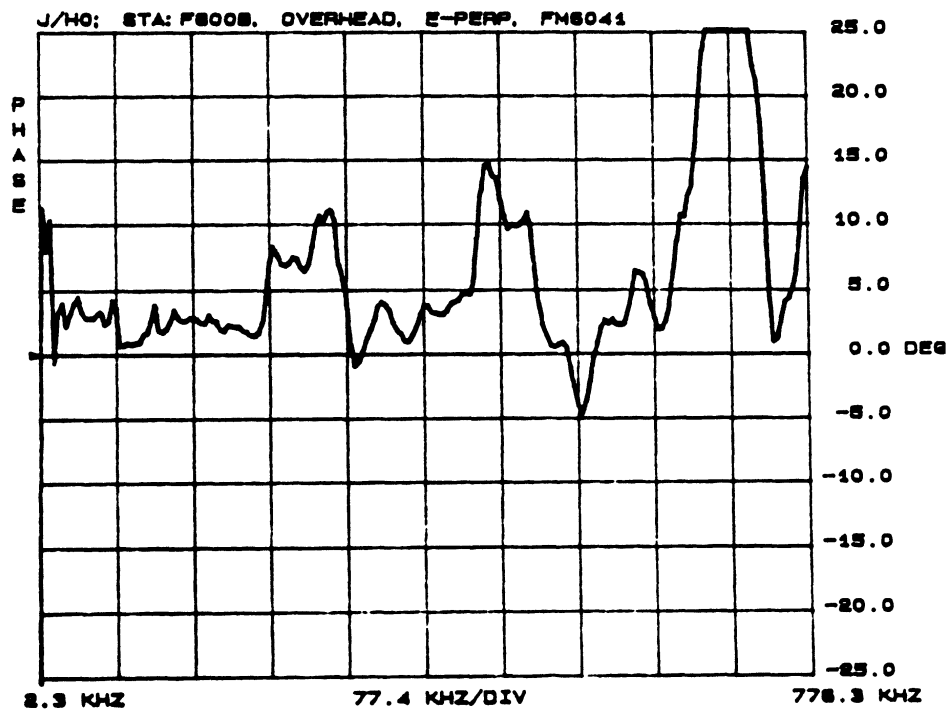
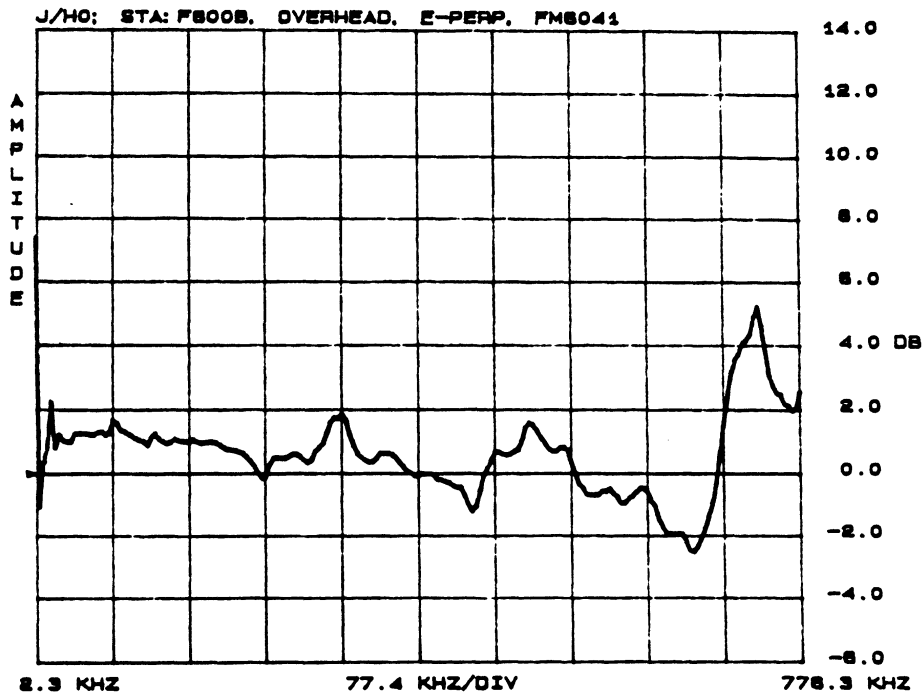


Plot 6. Current amplitude and phase at sta:F1350B, overhead incidence, E-parallel to fuselage; FM6025.

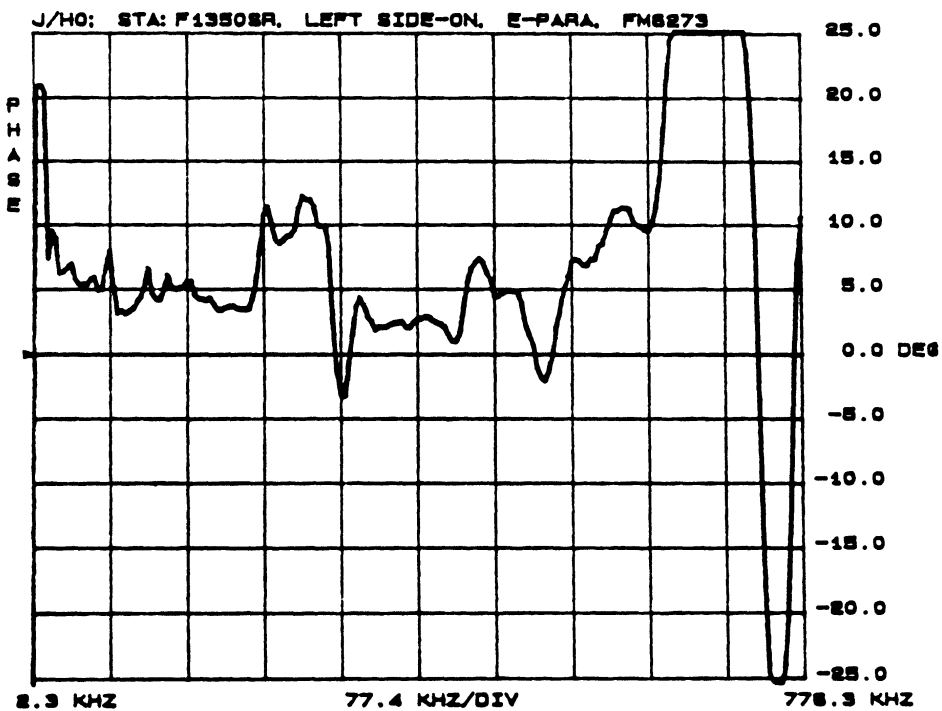
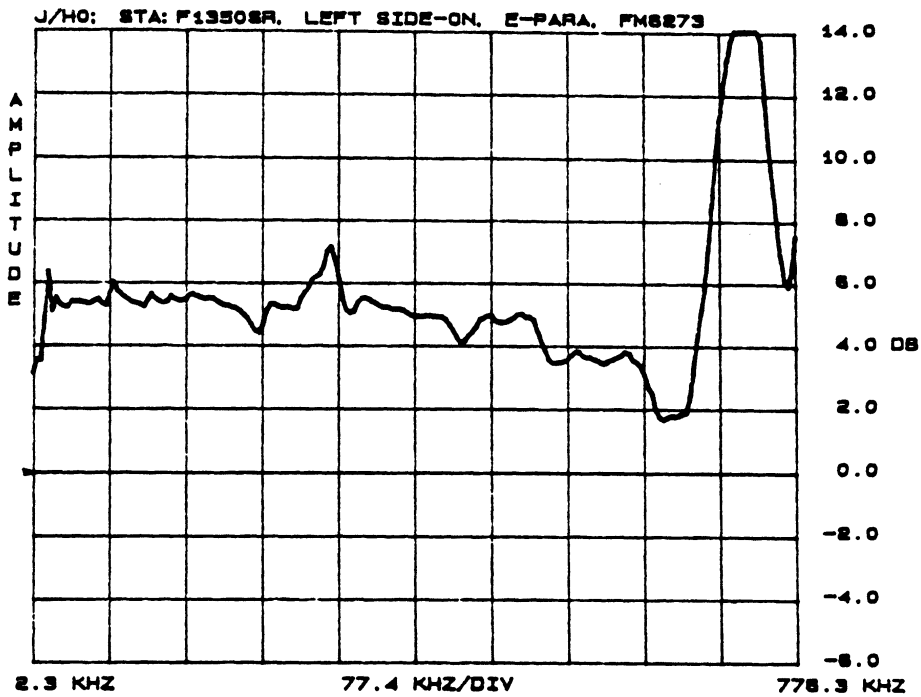




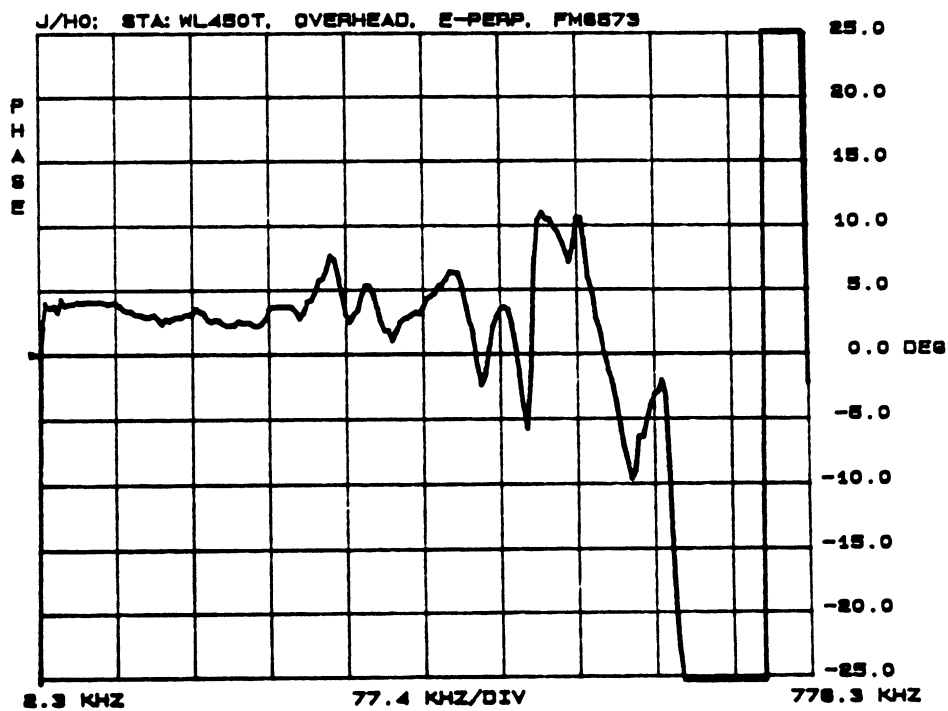
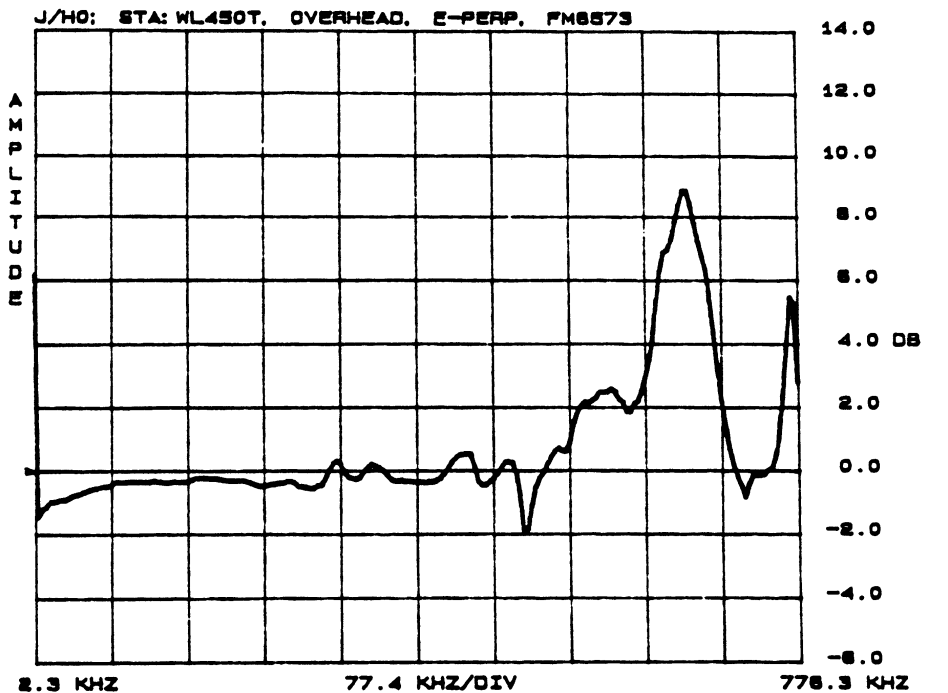
Plot 7. Current amplitude and phase at sta:F800T, overhead incidence, E-perpendicular to fuselage; FM6033.



Plot 8. Current amplitude and phase at sta:F800B, overhead incidence, E-perpendicular to fuselage; FM6041.



Plot 9. Current amplitude and phase at sta:F1350SR, left side-on incidence, E-parallel to fuselage; FM6273.



Plot 10. Current amplitude and phase at sta:WL450T, overhead incidence, E-perpendicular to fuselage; FM6573.